

Cite this: *Chem. Sci.*, 2019, **10**, 10723 All publication charges for this article have been paid for by the Royal Society of ChemistryReceived 12th September 2019
Accepted 11th October 2019DOI: 10.1039/c9sc04616j
rsc.li/chemical-science

Introduction

Selenium is often regarded as a toxic metalloid, but it is also an essential bioinorganic dietary micronutrient.^{1–3} For example, geographic regions with selenium-deficient soil display unusually high occurrences of conditions including Keshan and Kashin-Beck diseases in the population, which are both tied to a dietary scarcity of selenium.^{4,5} Dietary sources of selenium are typically selenomethionine (SeMet) and selenate salts (SeO_4^{2-}), which must pass through complex metabolic pathways prior to incorporation into selenium-containing biomolecules.⁶ In the body, selenium exerts function primarily as selenocysteine, often referred to as the 21st amino acid, which is incorporated into and gives rise to the often unique reactivity of selenoproteins.⁷

Twenty-five selenoproteins have been identified in humans and fall into several main categories. These categories include glutathione peroxidases (Gpx), which scavenge harmful peroxide species, thioredoxin reductases (TrxR), which regulate thiol-disulfide redox homeostasis, iodothyronine deiodinases (DIOs), which regulate thyroid hormone equilibria, and specialized selenoproteins that exhibit alternative functions, such as protein folding and selenium transport.³ Selenium-

deficient environments often result in the preferential expression of these proteins, whereas selenium-rich environments result in the upregulation of selenium excretion pathways to mitigate selenium toxicity.⁸ Many of these pathways are hypothesized to proceed through the intermediate formation of hydrogen selenide ($\text{H}_2\text{Se}/\text{HSe}^-$), which is an important yet elusive small biomolecule of interest (Fig. 1).⁹

A common approach to increase the bioavailability of selenium is to use exogenous synthetic selenium-containing small molecules. For example, the organoselenium compound ebse-lenn mimics the behavior of glutathione peroxidase and exhibits cytoprotective, anti-inflammatory, and antioxidant effects.^{10,11} Similarly, the glutathione-mediated reduction of selenite (SeO_3^{2-}) to elemental selenium is thought to proceed through a selenodiglutathione (GS-Se-SG) intermediate en-route to a selenopersulfide (GS-SeH), which subsequently either decomposes to GSH and Se^0 or is converted to H_2Se through both enzymatic and non-enzymatic pathways.^{12,13} More recently, the hydrolysis of phthalic selenoanhydride was used to generate reactive selenium species (RSeS) to examine the differential synergies of these compounds with H_2S and GSH in radical scavenging.¹⁴ In this investigation, H_2Se release was proposed during hydrolysis but was not observed directly in the experiments.

Interest in developing chemical tools for investigating H_2Se and related RSeS has grown in the last few years, with new investigations into the molecular recognition of HSe^- in synthetic host-guest systems¹⁵ and with the advent of first-generation fluorescent probes for H_2Se detection.^{16,17} In part, these investigations are motivated by potential roles of

Department of Chemistry and Biochemistry, Materials Science Institute, Institute of Molecular Biology, University of Oregon, Eugene, OR 97403, USA. E-mail: pluth@uoregon.edu

† Electronic supplementary information (ESI) available: Synthetic details, NMR spectra, HPLC experiments, crystallographic information. CCDC 1953366. For ESI and crystallographic data in CIF or other electronic format see DOI: 10.1039/c9sc04616j



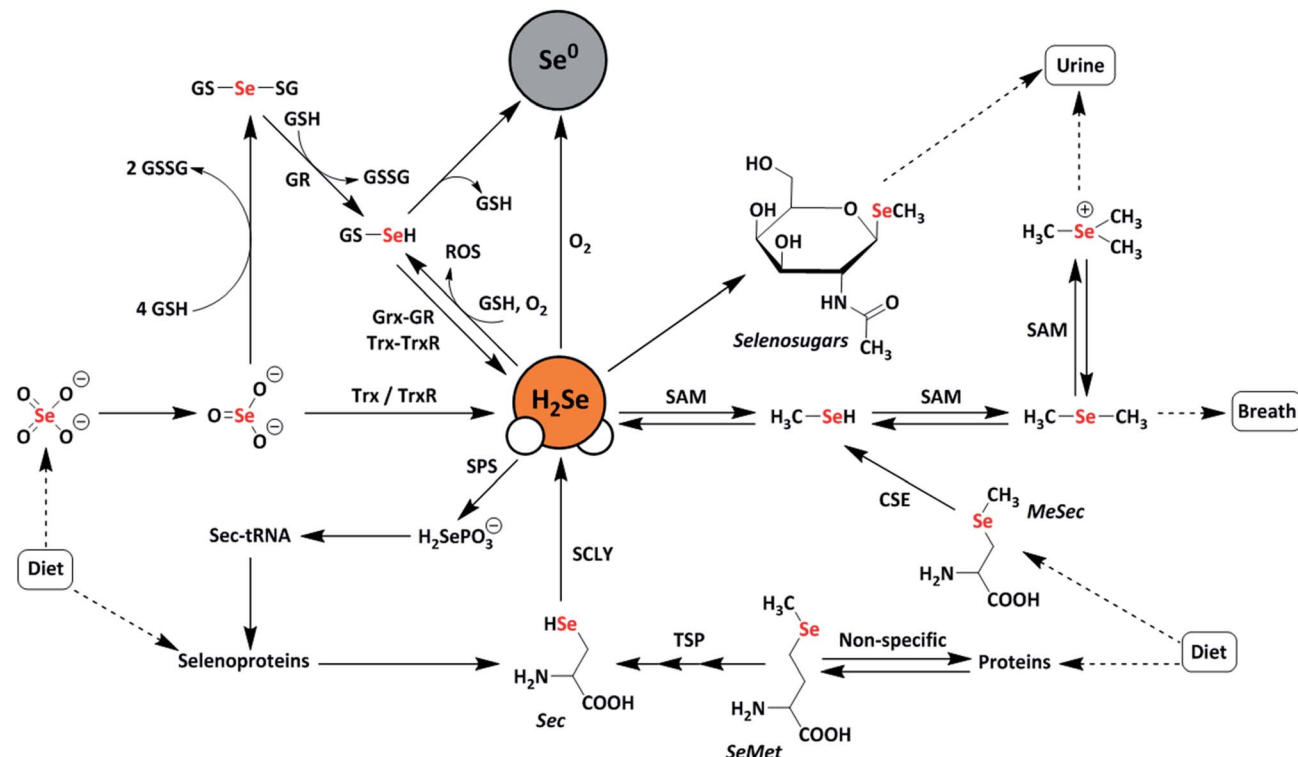


Fig. 1 Schematic representation of metabolic pathways of dietary selenium compounds including various reactive selenium species. Selenate (SeO_4^{2-}), selenite (SeO_3^{2-}), selenophosphate ($\text{H}_2\text{SePO}_3^-$), selenocysteine (Sec), selenomethionine (SeMet), methylselenocysteine (MeSec), thioredoxin (Trx), thioredoxin reductase (TrxR), glutaredoxin (Grx), glutathione reductase (GR), glutathione (GSH), glutathione (GSSG), selenodiglutathione (GSSeSG), glutathioselenol (GSSeH), selenophosphate synthetase (SPS), selenocysteine lyase (SCLY), S-adenosylmethionine (SAM), transsulfuration pathway (TSP), elemental selenium (Se^0), and reactive oxygen species (ROS).

selenides in treating conditions ranging from arsenic poisoning, in which toxic arsenic species can react with H_2Se to form readily-excreted products,^{18,19} to cancer, in which H_2Se can induce oxidative stress under normoxic conditions or reductive stress under hypoxic conditions in HepG2 cells, resulting in HMGB1 protein damage and ultimately apoptosis.²⁰ At physiological pH, almost all H_2Se exists as HSe^- due to the acidity of the diprotic form of H_2Se ($\text{p}K_a = 3.9$). The high redox activity and high nucleophilicity of $\text{H}_2\text{Se}/\text{HSe}^-$, when coupled with the relatively low biological selenium content ($\sim 0.2 \text{ mg kg}^{-1}$ in humans), make investigations into the biological roles of H_2Se difficult.^{21,22} Building from these past results and increased interest in biorelevant small RSeS, we viewed that well-characterized, synthetic small molecules that release H_2Se directly and under controlled conditions would provide a much-needed chemical tool for expanding research related to the chemical biology of selenium. Here we report the development and characterization of a hydrolysis-based small-molecule H_2Se donor and provide insights into the reaction mechanism and methods for direct H_2Se trapping.

Results and discussion

Drawing parallels to biological organosulfur chemistry, the last fifteen years have witnessed a surge in research related to hydrogen sulfide ($\text{H}_2\text{S}/\text{HS}^-$) as an important reactive sulfur

species and gasotransmitter.²³ Substantial efforts have focused on the development of small-molecule H_2S donors for delivery to biological environments.^{24–26} Although the structure and complexity of such systems have evolved significantly, an early and broadly-used example of such donors is the hydrolysis-activated donor GYY4137, which relies on the hydrolytic cleavage of P=S bonds to generate H_2S .²⁷ GYY4137 has been used in >200 publications to date (Web of Science) and exhibits

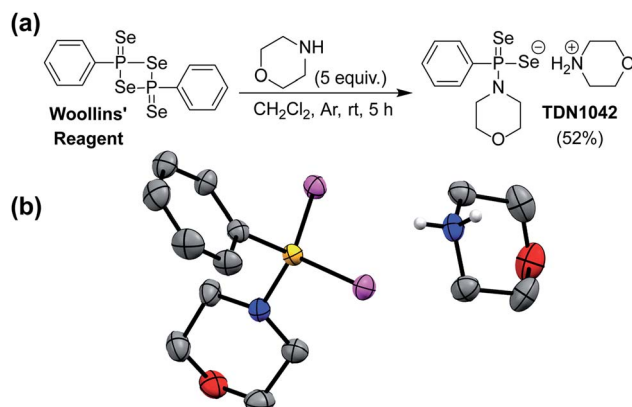


Fig. 2 (a) Synthesis of TDN1042 from Woollins' reagent. (b) ORTEP diagram (50% ellipsoids) of TDN1042. Hydrogen atoms, except those on the morpholinium nitrogen, are omitted for clarity.

anti-inflammatory, vasorelaxant, and anti-cancer as well as other effects in different biological models^{27–29} with diverse applications ranging from medicinal to agricultural science.^{30,31} Motivated by the broad utility of this approach to access H₂S donor motifs, we sought to use similar chemistry to generate well-defined H₂Se donors that are activated by P=Se bond hydrolysis. To prepare such a donor, we treated Woollins' reagent with an excess of morpholine, drawing parallels to the synthesis of GYY4137, to generate TDN1042 in moderate yield (Fig. 2a). The resultant product was characterized by ¹H, ³¹C {¹H}, ³¹P, and ⁷⁷Se NMR spectroscopy (Fig. S1–S4†). Single crystals suitable for X-ray diffraction were grown by layering hexane onto a solution of TDN1042 in CH₂Cl₂, which confirmed the molecular structure (Fig. 2b).

With TDN1042 in hand, we next evaluated its reaction chemistry by NMR spectroscopy. Initial studies using ³¹P NMR spectroscopy in wet DMSO-*d*⁶ revealed the clean conversion of TDN1042 to phenylphosphonic acid (PPA) as expected (Fig. 3a). We next monitored the hydrolysis in buffered aqueous solutions using quantitative ³¹P NMR spectroscopy with triethylphosphosphate (TEP) as an internal integration standard. In these experiments, we also observed clean conversion of TDN1042 (δ (³¹P) = 61 ppm) to the expected PPA hydrolysis product (δ (³¹P) = 12 ppm). To determine the effect of pH on this reaction, we

measured the rate of hydrolysis of TDN1042 (10 mM) in citrate buffer (50 mM) ranging from pH 3.0 to pH 6.0 in flame-sealed NMR tubes at ambient temperature (Fig. 3b). The resulting hydrolysis data (Fig. 3c) revealed an increase in rate at more acidic pH values, which is consistent with the expected hydrolysis mechanism. A similar pH dependence was observed for GYY4137 in a previous report,²⁷ although the experimental conditions and methods used to monitor rates and product conversions are too dissimilar to those used here for TDN1042 to make direct quantitative comparisons. This similarity in pH dependences does, however, suggest that TDN1042 could find utility in biological contexts much like GYY4137.

Having established that the hydrolysis of TDN1042 results in PPA formation, we next sought to confirm H₂Se release directly. To monitor H₂Se release, our goal was to trap H₂Se directly rather than use fluorogenic probes in case a reactive intermediate en-route to H₂Se release resulted in the activation of such systems. To accomplish this labeling, we used benzyl bromide (BnBr) as an electrophilic trapping agent and monitored the reaction by ³¹P and ⁷⁷Se NMR spectroscopy (Fig. 4a). On the basis of the proposed release mechanism of H₂Se from TDN1042, we expected that, akin to initial protonation, BnBr would initially alkylate the P=Se moiety, which would activate TDN1042 toward hydrolysis to release benzyl selenol (BnSeH) with subsequent alkylation by BnBr to generate dibenzyl selenide (Bn₂Se). By monitoring the reaction by both ³¹P and ⁷⁷Se NMR spectroscopy, we observed immediate formation of an intermediate (1) upon addition of BnBr and H₂O to a solution of TDN1042 in DMSO-*d*⁶ (Fig. 4b and c). Intermediate 1 exhibited a singlet in the ³¹P spectrum (δ = 69 ppm) with two sets of selenium satellites with different coupling constants (J_{P-Se} = 786 Hz, J_{P-Se} = 401 Hz). This coupling pattern is consistent with inequivalent selenium environments in 1 and is in contrast to the single set of selenium satellites seen in TDN1042 (δ (³¹P) = 61 ppm, J_{P-Se} = 671 Hz). Furthermore, the ⁷⁷Se NMR spectrum of 1 revealed both a doublet (δ = -129 ppm, J_{P-Se} = 786 Hz) and a doublet of triplets (δ = 354 ppm, J_{P-Se} = 401 Hz, J_{Se-H} = 11 Hz), which correspond to the P=Se and P-SeCH₂Ph moieties, respectively (Fig. 4e). As the reaction proceeded, the intensity of the δ = -129 and 354 ppm peaks decreased, with concomitant formation of PPA (δ (³¹P) = 12 ppm) in the ³¹P NMR spectrum. The ⁷⁷Se NMR spectrum revealed two Se-containing products, with a triplet at δ (⁷⁷Se) = 394 ppm and a pentet at δ (⁷⁷Se) = 330 ppm. The 330 ppm resonance corresponds to Bn₂Se, in which the selenium signal is split by two sets of benzylic protons. The 394 ppm resonance corresponds to dibenzyl diselenide (Bn₂Se₂), which was confirmed by comparison with an authentic Bn₂Se₂ sample (Fig. S13†). Formation of the diselenide is likely due to the auto-oxidation of BnSeH, which as has been observed previously.³² Taken together, these alkylation experiments support the mechanism of H₂Se release and provide mechanistic insights into the hydrolysis mechanism.

To definitively establish H₂Se release, we next performed experiments in which the electrophilic trapping agent was separate from the donor. For this investigation, we used 2,4-dinitrofluorobenzene (FDNB) as an electrophilic labeling reagent to trap the H₂Se released and volatilized into the

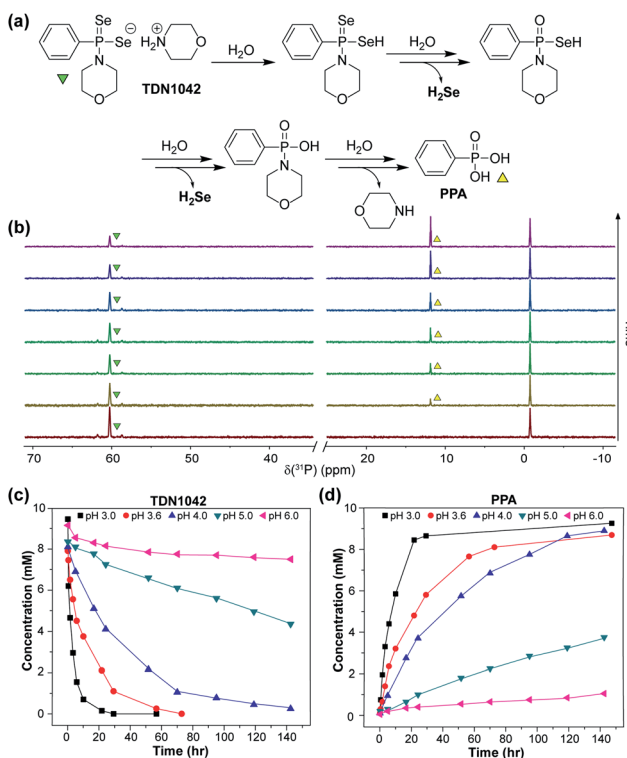


Fig. 3 (a) Proposed hydrolysis mechanism of TDN1042 resulting in H₂Se release. (b) ³¹P NMR spectra during the hydrolysis of TDN1042 showing the consumption of TDN1042 (61 ppm) and generation of PPA (12 ppm). (c) pH dependence of TDN1042 during the hydrolysis experiments. (d) pH dependence of PPA formation during the hydrolysis experiments. General conditions: 10 mM TDN1042 in 50 mM citrate buffer ranging from pH 3.0 to pH 6.0 at room temperature.



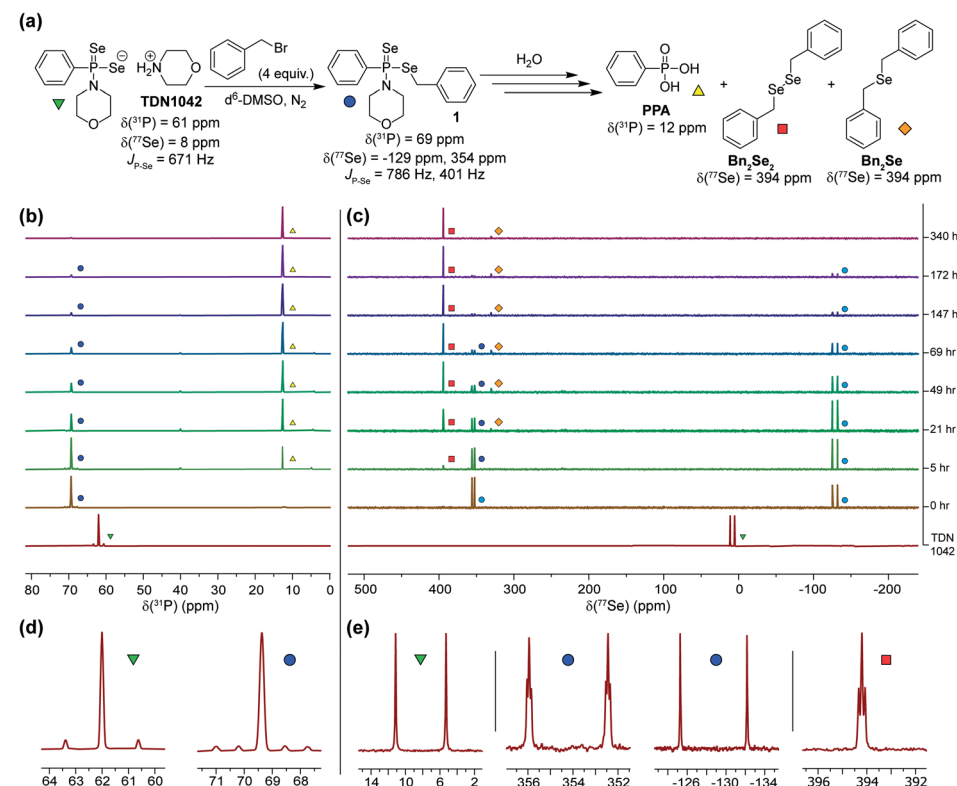


Fig. 4 (a) Proposed hydrolysis and trapping pathways. See Scheme S3† for a more detailed mechanism. (b) ^{31}P NMR spectra during alkylation and hydrolysis. (c) ^{77}Se NMR spectra during alkylation and hydrolysis. (d and e) Expanded regions of the ^{31}P and ^{77}Se NMR spectra highlight the observed coupling patterns.

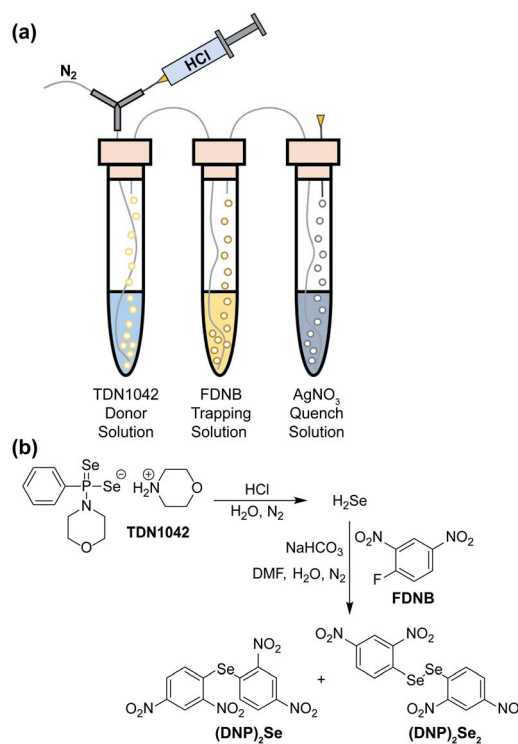


Fig. 5 (a) Experimental setup for volatilization and trapping of H_2Se with FDNB. (b) General reaction pathways for $(DNP)_2Se$ and $(DNP)_2Se_2$ formation.

headspace of the reaction apparatus.^{33,34} In these experiments, a vial containing an aqueous solution of TDN1042 was acidified with HCl and sparged with N_2 to help volatilize any H_2Se into the headspace, which was subsequently bubbled through a trapping solution containing a large excess of FDNB (Fig. 5a). A final solution containing $AgNO_3$ was used to scavenge any unreacted H_2Se . Using HPLC, we observed formation of both di(2,4-dinitrophenyl) selenide ($(DNP)_2Se$) and the corresponding diselenide ($(DNP)_2Se_2$) in the trapping solution (Fig. 5b and S14†), which is consistent with directly trapping H_2Se as well as the auto-oxidation process. The identity of the observed products was confirmed by comparison to authentic samples of $(DNP)_2Se$ and $(DNP)_2Se_2$ synthesized according to published procedures (Fig. S18†).³⁵ Taken together, these results confirm that TDN1042 releases H_2Se directly.

Conclusions

Here we report the development and characterization of the hydrolysis-based H_2Se donor TDN1042. Using multinuclear NMR experiments, we monitored the reaction pathway for H_2Se release and confirmed H_2Se generation using different electrophilic trapping methods. We anticipate that this well-characterized H_2Se donor will find utility in biological investigations into the roles of H_2Se and related reactive selenium species in the future and will facilitate the development of

chemical tools for further investigating H₂Se in chemical biology.

Conflicts of interest

There are no conflicts to declare.

Acknowledgements

This research was supported by the NSF (CHE-1454747) and Dreyfus Foundation. NMR capabilities in the UO CAMCOR facility are supported by the NSF (CHE-1427987, CHE-1625529). We would like to thank Dr Samantha N. MacMillan from the X-ray diffraction facility at Cornell University for crystal structure determination.

Notes and references

- 1 R. C. McKenzie, T. S. Rafferty and G. J. Beckett, *Immunol. Today*, 1998, **19**, 342–345.
- 2 L. Schomburg, U. Schweizer and J. Kohrle, *Cell. Mol. Life Sci.*, 2004, **61**, 1988–1995.
- 3 H. J. Reich and R. J. Hondal, *ACS Chem. Biol.*, 2016, **11**, 821–841.
- 4 J. S. Chen, Asia Pac, *J. Clin. Nutr.*, 2012, **21**, 320–326.
- 5 P. Sudre and F. Mathieu, *Int. Orthop.*, 2001, **25**, 175–179.
- 6 L. V. Papp, J. Lu, A. Holmgren and K. K. Khanna, *Antioxid. Redox Signaling*, 2007, **9**, 775–806.
- 7 D. L. Hatfield, P. A. Tsuji, B. A. Carlson and V. N. Gladyshev, *Trends Biochem. Sci.*, 2014, **39**, 112–120.
- 8 R. F. Burk and K. E. Hill, *Annu. Rev. Nutr.*, 2015, **35**, 109–134.
- 9 K. A. Cupp-Sutton and M. T. Ashby, *Antioxidants*, 2016, **5**, 42–59.
- 10 T. Schewe, *General Pharmacology: The Vascular System*, 1995, **26**, 1153–1169.
- 11 J. L. Wedding, B. Lai, S. Vogt and H. H. Harris, *Biochim. Biophys. Acta*, 2018, **1862**, 2393–2404.
- 12 H. S. Hsieh and H. E. Ganther, *Biochemistry*, 1975, **14**, 1632–1636.
- 13 J. Kessi and K. W. Hanselmann, *J. Biol. Chem.*, 2004, **279**, 50662–50669.
- 14 A. Kharma, A. Misak, M. Grman, V. Brezova, L. Kurakova, P. Barath, C. Jacob, M. Chovanec, K. Ondrias and E. Domínguez-Álvarez, *New J. Chem.*, 2019, **43**, 11771–11783.
- 15 H. A. Fargher, N. Lau, L. N. Zakharov, M. M. Haley, D. W. Johnson and M. D. Pluth, *Chem. Sci.*, 2019, **10**, 67–72.
- 16 F. P. Kong, L. H. Ge, X. H. Pan, K. H. Xu, X. J. Liu and B. Tang, *Chem. Sci.*, 2016, **7**, 1051–1056.
- 17 F. P. Kong, Y. H. Zhao, Z. Y. Liang, X. J. Liu, X. H. Pan, D. R. Luan, K. H. Xu and B. Tang, *Anal. Chem.*, 2017, **89**, 688–693.
- 18 H. J. Sun, B. Rathinasabapathi, B. Wu, J. Luo, L. P. Pu and L. Q. Ma, *Environ. Int.*, 2014, **69**, 148–158.
- 19 I. Zwolak, *Biol. Trace Elem. Res.*, 2019, 1–20.
- 20 X. H. Pan, X. X. Song, C. Wang, T. T. Cheng, D. R. Luan, K. H. Xu and B. Tang, *Theranostics*, 2019, **9**, 1794–1808.
- 21 H. A. Schroeder, D. V. Frost and J. J. Balassa, *J. Chronic Dis.*, 1970, **23**, 227–243.
- 22 M. Navarro-Alarcon and C. Cabrera-Vique, *Sci. Total Environ.*, 2008, **400**, 115–141.
- 23 R. Wang, *FASEB J.*, 2002, **16**, 1792–1798.
- 24 S. D. Zanatta, B. Jarrott and S. J. Williams, *Aust. J. Chem.*, 2010, **63**, 946–957.
- 25 M. M. Cerdá, T. D. Newton, Y. Zhao, B. K. Collins, C. H. Hendon and M. D. Pluth, *Chem. Sci.*, 2019, **10**, 1773–1779.
- 26 C. M. Levinn, A. K. Steiger and M. D. Pluth, *ACS Chem. Biol.*, 2019, **14**, 170–175.
- 27 L. Li, M. Whiteman, Y. Y. Guan, K. L. Neo, Y. Cheng, S. W. Lee, Y. Zhao, R. Baskar, C. H. Tan and P. K. Moore, *Circulation*, 2008, **117**, 2351–2360.
- 28 L. Li, M. Salto-Tellez, C. H. Tan, M. Whiteman and P. K. Moore, *Free Radical Biol. Med.*, 2009, **47**, 103–113.
- 29 Z. W. Lee, X. Y. Teo, E. Y. W. Tay, C. H. Tan, T. Hagen, P. K. Moore and L. W. Deng, *Br. J. Pharmacol.*, 2014, **171**, 4322–4336.
- 30 G. L. Meng, J. Wang, Y. J. Xiao, W. L. Bai, L. P. Xie, L. Y. Shan, P. K. Moore and Y. Ji, *J. Biomed. Res.*, 2015, **29**, 203–213.
- 31 J. M. Carter, E. M. Brown, J. P. Grace, A. K. Salem, E. E. Irish and N. B. Bowden, *PLoS One*, 2018, **13**, e0208732.
- 32 A. R. M. de Oliveira, L. Piovan, F. Simonelli, A. Barison, M. D. C. Santos and M. B. M. de Mello, *J. Organomet. Chem.*, 2016, **806**, 54–59.
- 33 H. E. Ganther and R. J. Kraus, *Anal. Biochem.*, 1984, **138**, 396–403.
- 34 H. E. Ganther and R. J. Kraus, *Methods Enzymol.*, 1987, **143**, 32–38.
- 35 D. F. Twiss, *J. Chem. Soc.*, 1914, **105**, 1672–1678.

